2020 IEEE/RSJ International Conference on Intelligent Robots and Systems (IROS)
October 25-29, 2020, Las Vegas, NV, USA (Virtual)

Utilizing Sacrificial Molding for Embedding Motion Controlling Endostructures in Soft Pneumatic Actuators

Ajinkya Bhat
NUS Graduate School for Integrative Sciences and Engineering
National University of Singapore
Singapore
ajinkyab@u.nus.edu

Raye Chen-Hua Yeow
Department of Biomedical Engineering
National University of Singapore
Singapore
rayeow@nus.edu.sg

***Abstract*—The field of soft robotics has evolved as a domain for developing light, compliant and safe actuators. However, one of the challenges in the field is the lack of repeatable fabrication techniques as well as customizability that restricts the application of soft robots. We present a fabrication technique using sacrificial molding to fabricate pneumatic channels that are repeatable and less prone to variability. This technique enables the monolithic fabrication of actuators which eliminates conventional failure modes such as delamination. We then use embedded endostructures manufactured using Fused Deposition Modelling (FDM) 3D printers to customize the behavior of bending actuator by altering local mechanical characteristics. Finite element analysis (FEA) was used as a tool to tune the choice of materials and the geometry of the 3D printed layers based on the required application. We analyze the effect of the mechanical properties of the endostructures on actuator behavior and its utility in improving customizability. We analyzed the behavior of actuators with a variety of endostructures using visual markers. As predicted by the FEA and Euler-Bernoulli beam theory, the behavior of the actuators was seen to be influenced by the mechanical properties of the endostucture. Thus, we present a new methodology for tuning the mechanical properties of Soft Pneumatic Actuators (SPAs), which is simple and efficient to predict as well as easy to execute.**

***Index Terms*—Soft Robotics, Pneumatic Actuators, Soft Robot Fabrication, Mechanical Programming, Finite Element Analysis**

I. Introduction

Soft robotics has evolved over the last decade as a means for producing compliant and safe robotic manipulators, especially for applications that involve interactions with humans [1], [2]. However, the mainstream adoption of soft robots has been limited due to the lack of repeatable fabrication methods and large variance in fabricated design. Some of the limitations of current soft robots include the fact that it is difficult to design complex structures and reproduce internal geometry consistently [2]–[4]. Thus, the mechanical characteristics are bound to vary due to the variability and lack of reproducibility.

Silicone has proved to be a very popular material for the fabrication of soft actuators over the last two decades due to its low stiffness and weight, bio-compatibility, and ability to withstand large strains [5]. Silicone actuators were molded in two pieces [6] which led to weaknesses that lead to delamination, a failure mode where the shear force acting on the separately cured pieces leads to them being pulled apart. Recent improvements have resolved this issue to some extent using sacrificial molding. Sacrificial molding using lost wax method was used in [3], [7] to enable fabrication of soft elastomeric actuators that could resist delamination. Sacrificial molding has also been used for the fabrication of micro-channels [8], [9] to enable more complex micro-channel designs. Methods such as rotational casting [10] and silicone three-dimensional printing [11] have been developed but require complex parameter tuning or specialized machines. In this manuscript, we use a negative mold material that can be dissolved in a later stage of fabrication that allows us to fabricate the pneumatic channel in one piece, leading to a consistent and stronger fabrication, with low propensity for human skill-based errors.

Since pneumatically powered soft robots are essentially unconstrained continuums, they have to be constrained in certain locations to achieve specific motions, such as bending or twisting. These constraints dictate the macroscopic behavior of the robot. Some methods of controlling the behaviors involve using constraints such as using granular jamming both internally [12], [13] and externally [14] or external shells for reinforcement [2]. External constraints such as crustacean inspired exoskeletons [4] and skins [15] have also been explored. The most common method of controlling the behavior of soft elastomeric robots is using fiber reinforcement [16]–[19]. Actuators based on elastomers were shown to have varied characteristics by changing their fiber reinforcement pattern [17]. A kirigami exoskeleton can be used in addition to the fibers to achieve frictional properties for crawling [20]. Fiber reinforcement remains an option but it inherently impedes the motion and thus higher pressure is required [1] at the advantage of higher force output. Whereas this is a circumferential constraint, local constraints allow for tuning of properties as well, without making the entire actuator so stiff as to significantly increase required pressure [21]. Conventional pneunets [6] involve using a material such as paper to provide a higher stiffness to allow for bending, but the fabrication is complex, lacks customizability and is prone to errors due to high degree of human skill involved. In this manuscript, we propose a novel way of looking at constraining soft robots using embedded internal structures, called endostructures. Inspired by the endoskeletons that biological systems such as echinoderms possess that allow for continuum motion, these embedded endostructures enable us to control the behavior of the soft robot using a varied compliance pattern, which is achieved by changes in design or material of the endostructure. Unlike [22], [23] where the joints were active and controlled by heat, we use passive joints whose properties are tuned using FEA.

II. Design and Fabrication

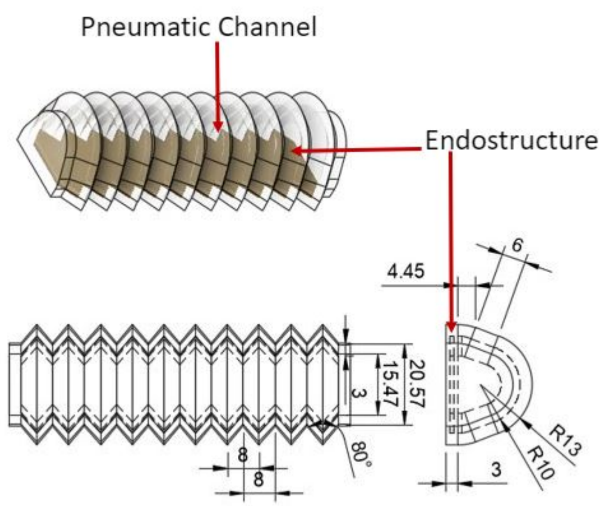

Fig. 1: The design of the actuator. The thickness of the design is 3mm . The endostucture is embedded in the bottom layer, seen as a beige strip. The pneumatic channel is in centre. All dimensions are in mm

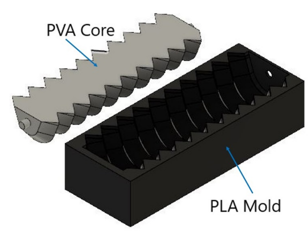

(a) Step 1: Fabrication of the PVA negative and the PLA Mould using FDM 3D Printing

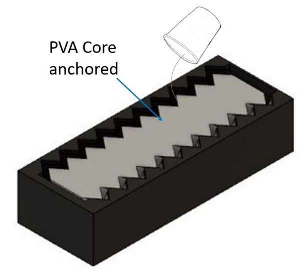

(b) Step 2: The PVA is locked inside the mould and elastomer is poured over it

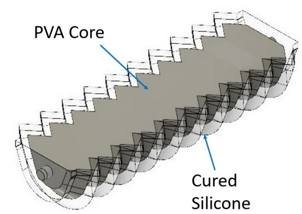

(c) Step 3: The cured part is removed

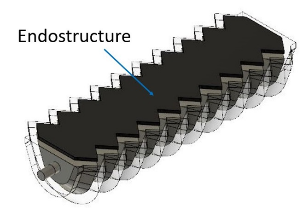

(d) Step 4: The endostructure is locked in place using an adhesive

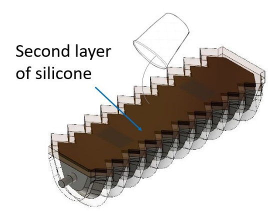

(e) Step 5: Elastomer is poured over the locked endostructure

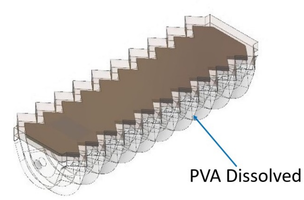

(f) Step 6: The PVA negative is dissolved to leave the final fabricated part

Fig. 2: Fabrication Process of Embedded Endostructure Soft Pneumatic Actuators (EESPAs)

A. Actuator Design

The design of the Embedded Endostructure Soft Pneumatic Actuators (EESPAs) is described in Fig. 1. The design consists of half-circle cross-section with corrugated walls with a central pneumatic channel, derived from an accordion-type design. The material thickness for the elastomer is 3mm. The section at the bottom represents the location of the embedded endostructure. The gap varies for the other endostructures presented later, due to the difference in dimensions. The design of the body of the actuator and the pneumatic channel remains the same. The actuators are designed for bending with positive pressure. A 4mm diameter air inlet is made during the fabrication process for inserting a tube to apply the pressure.

B. Single piece fabrication using water-soluble negative molds

We use the idea of sacrificial molding to create repeatable pneumatic channels and enable consistent fabrication. The sacrificial negative is made of Polyvinyl Alcohol (PVA), a water-soluble material that is printable on an FDM 3D Printer (Ultimaker 3, Ultimaker, Utrecht, Netherlands). The manufacturing using an FDM 3D printer provides a higher degree of repeatability along with the added advantage of being able to customize the design easily. The fabrication method mainly involves the following steps as shown in Fig. 2. The PLA outer mold and the PVA negative are printed using an FDM 3D Printer (Fig. 2a). The PVA negative is fixed inside the PLA. Dragonskin-10 (Smooth-On, Macungie, PA, USA) is mixed in a 1:1 ratio using a mixer (ARE-10, Thinky, USA) and degassed using a vacuum chamber to remove air bubbles. The elastomer is poured around the negative (Fig. 2b). The elastomer with the PVA inside is cured in an industrial oven at 50°C for 30 minutes. The cured first stage of the actuator is removed from the stage 1 mold (Fig. 2c) and the endostructure is attached to the surface using an adhesive (Fig. 2d). The purpose of the adhesive is to keep the part in place when a subsequent layer of silicone is poured over it in the second stage mold (Fig. 2e). The cured actuator with the negative is then removed from the second stage mold, and placed in an ultrasonic cleaner (Shesto, Watford, United Kingdom) to dissolve the PVA negative. Water temperature is set to 50° C to speed up the dissolution (Fig. 2f). Following the ultrasonic cleaning stage, the actuator can have an inlet attached where a hole was left during fabrication. Since the endostructure is completely embedded in between the two silicone layers, no relative motion is observed between the endostructure and the silicone. The embedding means that no bonding is required between the silicone and the endostructure, opening up possibilities of using a variety of materials other than those shown in this manuscript.

III. Controlling actuator behavior with the use of embedded endostructures

Strain limiting layers have been commonly used to control the bending of soft actuators: both silicone-based [16], [17] and fabric-based [1], [24]. The purpose of this layer is to generate unbalanced forces to drive the actuator motion to perform a motion, such as bending instead of expanding uniformly. In this manuscript, we present an endostructure that can be used in place of these conventional strain limiting layers to achieve the desired motion.

The 3D printed endostructures are mainly fabricated from thermoplastic polyurethane (TPU) (Shore Hardness 95A) from Ultimaker, on the Ultimaker 3 Fused Deposition Modelling (FDM) 3D printer. This material was chosen for its shore hardness- the 95A shore hardness means that the material becomes almost inextensible at a 2mm thickness, while still maintaining its bending capability. Also, since the material is still much stiffer than the used silicone, Dragonskin-10 (Shore Hardness 10A), the composition can produce the differential strain that is required for the pre-programmed motions. A composite endostructure, such as one made of a TPU and PLA can also be manufactured using dual extrusion, thus making the method quite versatile. We demonstrate this versatility in the following sections, using sole TPU structure with a variable thickness, as well as a TPU-PLA hybrid, which is planar. The former can be seen to control the motion due to the variance in mechanical properties due to thickness, while the latter influences the motion due to the effect of the properties of the individual materials in the composite.

A. Controlling bending profiles of EESPAs

We demonstrate how these endostructures can be used with the same pneumatic channel design to achieve different sets of motions. We use four different designs for the endostructures: A planar TPU structure (referred to as simple hereon), a TPU structure with extrusions in two places (referred to as segmented hereon), A TPU-PLA hybrid and a TPU structure with a gradient. Fig. 3 to 6 shows that the EESPA with the same air channel with different endostructures bends in different ways. In Fig. 3, the simple EESPA can be seen to bend in an almost uniform way, as expected. The TPU-PLA endostructure in Fig.4 has the stiffer PLA restrict the motion due to its higher stiffness, making the actuator bend less in the corresponding section. A similar effect is seen in the segmented EESPA, with two extrusions 5- the higher stiffness restricts motion. Finally, the EESPA with the gradient 6 is seen to slightly curl towards its far end, which has a less stiff (thinner) endostucture.

The choice of material or materials for the endostructure is reliant on the type of motion to be achieved. For example, for bending actuators, the ideal endostructure would have low linear expansion and low resistance to bending. Thus, structures such as thin sections of TPU, non-stretchable fabric, or a composite TPU-PLA structure that does not stretch but allows for flexion in certain positions could be used. In the case of an actuator that requires the expansion, a material or structure that allows for it, such as stretchable fabric, would be a good choice. This customizability will allow for rapid tweaking of actuator designs by merely changing the design of the programming layer.

B. Tuning endostructure properties using finite element analysis as a tool

Finite element analysis (FEA) was used as a tool to customize the bending behavior of the actuators before fabrication. FEA based methods have been used to inform designs in literature [2], [6], [25], [26] and have been a popular approach of late as an alternative or complement to mathematical models. FEA provides an idea of the degree of bending and the distribution of stress and strain that can be achieved using a particular endostructure, following which the properties of the endostructure can be tweaked for a particular application. The model used was a reduced version of the actuator, with the air inlet, removed for simplicity.

We used a three-term Yeoh Model for modeling the Dragonskin-10 as a hyperelastic material as described in [27]. The TPU was modeled as a linear elastic material with Young's Modulus of 26kPa as per the manufacturer datasheet and a Poisson's ratio of 0.49. Abaqus (Dassault Systemes, France) was used for the finite element analysis. The PLA was modeled using manufacturer parameters as well- Young's Modulus of 2.3GPa and Poisson's ratio of 0.3. A solid tetrahedral quadratic element type with hybrid formulation (C3D10H) was chosen for the simulation to account for the large deformations and the hyperelastic properties of the materials used. The actuators are anchored at one end using an encastre boundary condition, and the inner face of the silicone has pressure applied to it to simulate air pressure. The actuator was assembled using the components which were the main body (DS-10), endostructure (TPU or TPU+PLA) and the final layer of silicone (DS-10). The parts were assembled using a tie constraint to represent the fact that there is no relative motion between the parts during actuation.

We used FEA to view the distribution of the stress in the endostructure to better tune the properties. Changing the structure as well as material of the endostructure can be seen

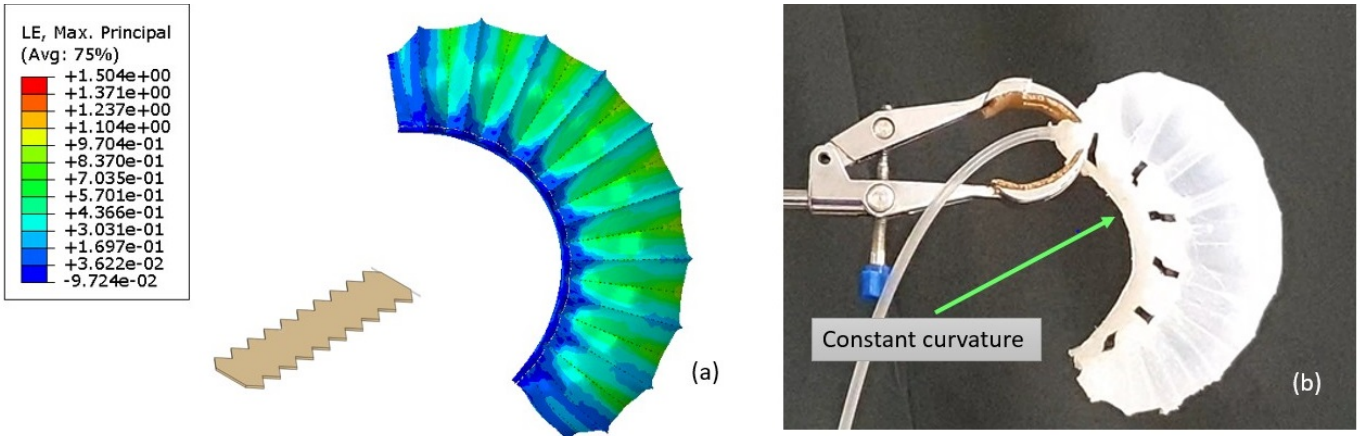

Fig. 3: A bending actuator with a planar embedded TPU endostructure. The bending is seen to be almost uniform. (a) shows FEA with strain distribution, (b) shows experimental prototype

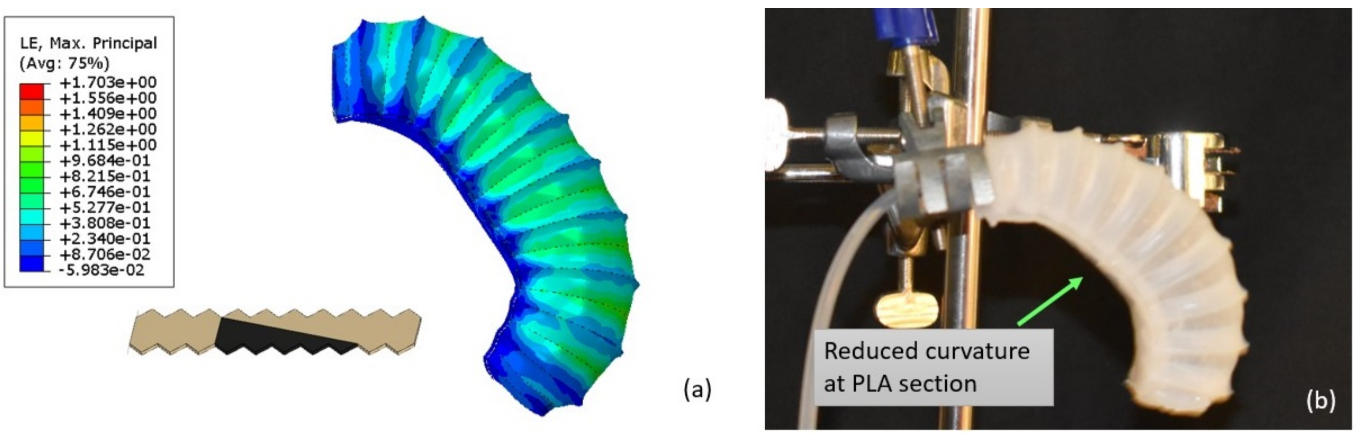

Fig. 4: A bending actuator with a TPU-PLA Endostuture. The central PLA part (black shade) shows reduced bending. (a) shows FEA with strain distribution, (b) shows experimental prototype

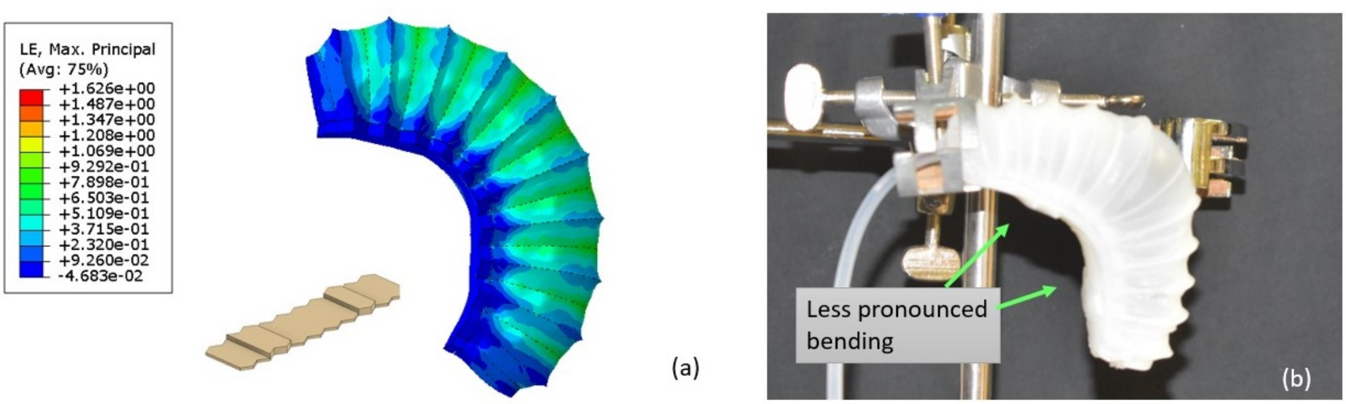

Fig. 5: A bending actuator with a embedded TPU endostructure with two extrusions. The part of extrusions shows lower bending and the corresponding part of the pneumatic channels shows perceivably higher expansion. (a) shows FEA with strain distribution, (b) shows experimental prototype

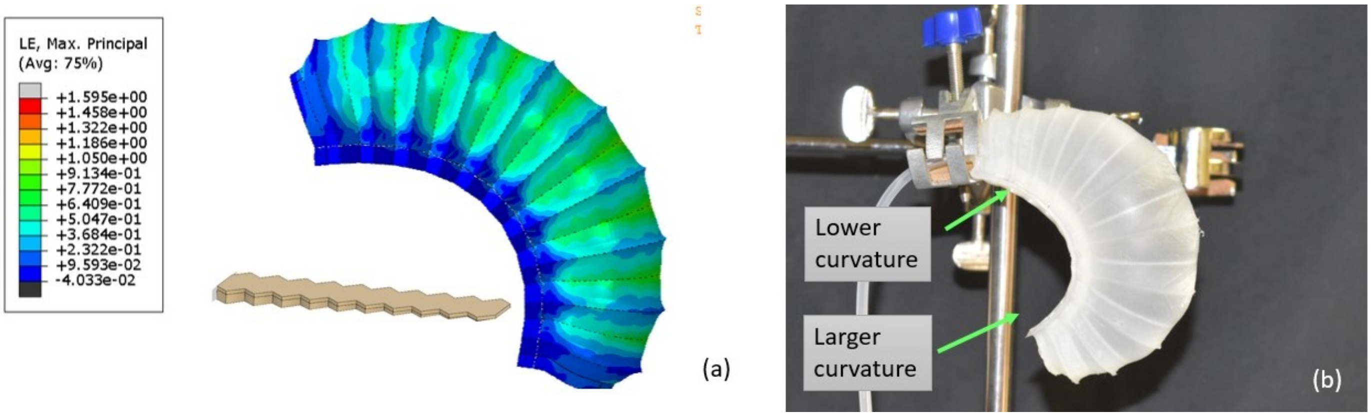

Fig. 6: A bending actuator with an embedded TPU endostructure with a gradient. The part of lower thickness (far end) shows much greater bending than the part close to the anchored side. (a) shows FEA with strain distribution, (b) shows experimental prototype

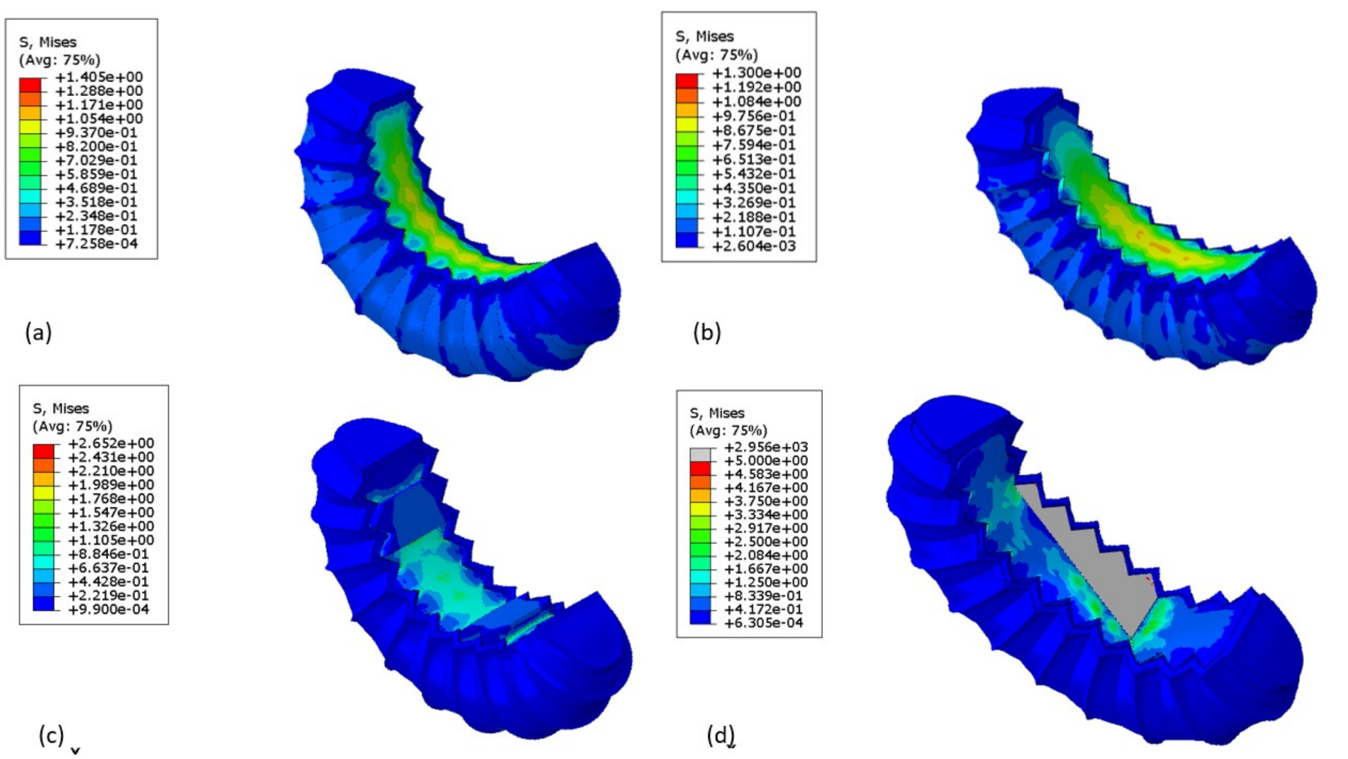

Fig. 7: Finite Element Analysis of the actuators at 15kPa with the final silicone layer removed to show the Von Mises stress distribution in the embedded endostructure. All stress is expressed in MPa. (a) Simple Actuator has a uniform stress distribution leading to constant curvature. (b) Gradient Actuator shows higher Von Mises stress towards the unanchored side, which in thinner leading to higher deformation. (c) Segmented Actuator shows higher Von Mises stress at the weaker central part, showing that the extrusions function as reinforcements to a bending beam. (d) The PLA section of the PLA-TPU hybrid has much higher stress but restricts the deformation due to its significantly higher Young’s Modulus.

to influence the stress in the endostructure, which in turn influences the properties of the actuator as a whole. Fig. 7 shows the effect of the changes in the endostructure design on the stress concentrations in the endostructure, and the corresponding effect on the behavior in the actuator. All stress is expressed in MPa.

Fig. 7 shows the stress distribution in the endostructures in the actuators. The actuators are anchored at the left end. Fig. 7a shows the Von Mises stress distribution in a planar TPU structure. As seen, the stress is distributed quite evenly along the surface, leading to almost a constant curvature at the output. In Fig.7b, the endostructure with the gradient, it can be seen that the stress is higher in the part of the endostructure with a lower thickness (towards the right). Thus, the thinner part shows a higher radius of curvature. Fig. 7c shows that the programmed endostructure has higher stress in the less thick (unreinforced) central section, which leads to greater bending in that section. Fig. 7d shows that the PLA takes a large proportion of the stress, but its extremely high Young's Modulus means that the deformation is heavily restricted. Thus, the actuator curls at the unreinforced far end.

The above observations can be explained using the stress equation from the Euler-Bernoulli Beam theory. The stress in a bending beam can be given by :

$$\sigma = \frac{My}{I} \tag{1}$$

where M is the moment of inertia about the neutral axis, y is the perpendicular distance to the neutral axis and I is the area moment of inertia. Additionally,

$$I = \frac{bh^3}{12} \tag{2}$$

where b is the base width, that is constant for all the parts, and h is the height of the part.

Approximating the behavior endostructure to a bending beam, we can use the above equations to explain the FEA and experimental results. The area moment of inertia in the case of the gradient actuator increases sharply at the thicker end due to an increase in h, leading to lower stress in that end. In the case of the actuator with two extrusions (referred to as segmented), a similar effect occurs. Since these two designs and the simple uniform design use the same single material, a change in stress profiles is sufficient to predict a change in deformation. In case of the PLA-TPU hybrid, the stress induced in the PLA is indeed higher, but simply not enough to cause bending due to its Young's Modulus being higher by a large factor.

IV. Quantitative study using visual markers

This section describes the quantitative analysis of the actuators for two-dimensional bending using Tracker, a video analysis tool from Open Source Physics. Colored markers are placed on the actuators at predetermined locations as shown in Fig. 8. The position is kept close to the bottom surface to minimize the effect due to the expansion of the pneumatic channels. The actuators are then given a pressure input from 0 kPa up to 20 kPa in steps of 5kPa. The video of the motion is recorded and processed at the point of static equilibrium. Marker positions are recorded to see the degree of bending at individual locations. Fig. 8 shows one such experiment for brevity.

The marker positions describing the bending profile of each actuator are analyzed using Tracker, a software for 2D analysis and presented in Fig. 9. The data can then be imported into MATLAB (Mathworks, MA, USA) for plotting. The origin offset is adjusted and the markers at each pressure are plotted using the corrected X and Y coordinates. We observe that compared to the simple planar structure, the gradient leads to higher curvature at the far end, which has a thinner endostructure profile than the anchored end. The TPU programmed structure is seen to bend in places of low thickness as well, although this is prominent only at higher pressure. The PLA structure is shown to also restrict the bending due to its high stiffness, as expected. Since the PLA-TPU and the "segmented" TPU structure as a whole are stiffer, the bending achieved at the same pressures is seen to be smaller. The trends support the predictions from the FEA.

V. Discussion

In this manuscript, we presented a method for fabricating SPAs using sacrificial molding using PVA, which is repeatable due to the negative being 3D printed. The actuators' only failure mode is seen to be due to weaknesses due to air bubbles that may be formed when molding. To make the actuator more resilient, we recommend having a wall thickness of at least 3mm. This is seen to provide a large enough gap for the air to escape in the molding process described in Fig.2. We also presented a method for controlling the behavior of soft pneumatic actuators using embedded endostructures to fabricate EESPAs. We achieve higher deformations at lower pressures than fiber-reinforced actuators [16], [17]. In addition, despite using a stiffer silicone, we achieve large deformations compared to actuators with external constrainers using Ecoflex-0030 [2]. The tradeoff, however as compared to these actuators is that due to lack of constraining elements, the actuator can only reach pressures upto 40kPa on average before showing signs of failure. The mechanical properties of the endostructures can be modified at will using a combination of materials, or different designs, which provides versatility. We demonstrated that FEA can be used as a tool to tune these characteristics.

Due to the use of the PVA negative, the EESPA is fabricated in a single piece. It must be noted here that, this works just as well if the primary pneumatic channel is isolated and subsequent features are then integrated in the following stages. Certain materials, such as fabrics, that have an affinity to silicone can be molded in a single stage. In our experiments, when we attempted to fabricate the channel with the 3D printed embedded endostructure in one stage, we observed the endostructure pop out at high deformations. This is due to the fact that the materials, especially TPU have very little

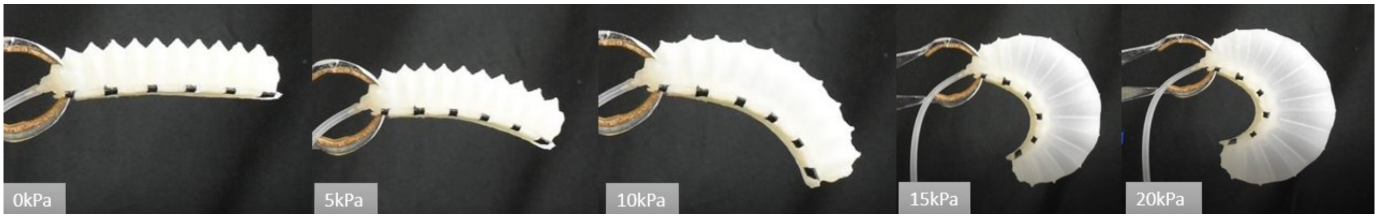

Fig. 8: Procedure for the actuator test using Tracker. Black markers are glued using silicone adhesive and the actuator inflation is recorded at a step of 5kPa from 0 to 20kPa. The snapshot is recorded 10 seconds after no visible movement is seen and assumed to be static equilibrium. The figure shows the gradient type actuator.

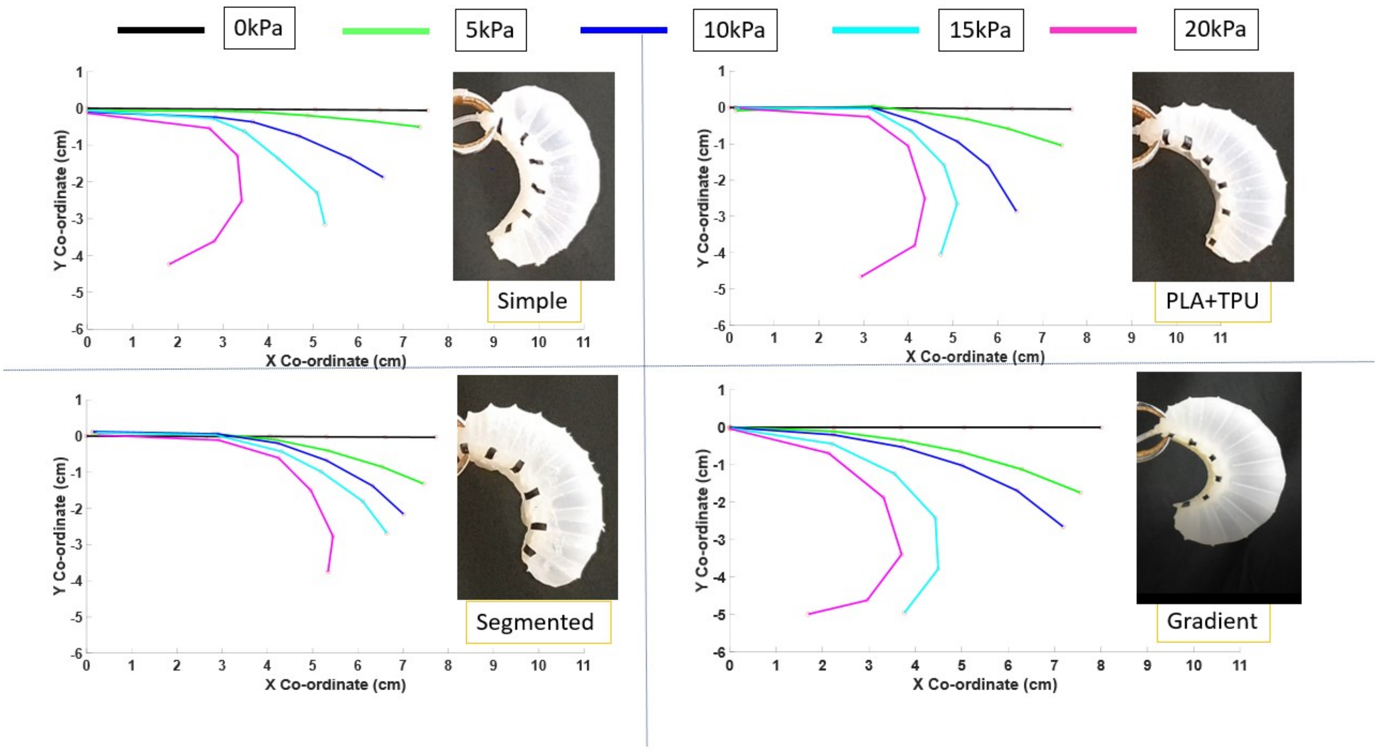

Fig. 9: Graphical Representation of the bending profiles at the recorded pressures at static equilibrium. A common trend is seen that the deformation is reduced at the fixed end, possibly due to . The curvature of the segmented type and PLA-TPU hybrid type was restricted in the stiff sections. The gradient type had high curvature at the unconstrained far end, which is thinner.

affinity to silicone, leading to detachment at high deformations. Fabrication of the pneumatic channel, in either case, is in a single stage, which eliminates the complexities in aligning the two separately molded parts and reduces the human element involved in the fabrication process, leading to better repeatability and no risk of failure by delamination [3], [7].

The above mentioned fabrication technique does come with a drawback that the PVA is non-reusable, as it dissolves. However, this is a small limitation, as the PVA is often printed between a 10-20% density to allow for quick dissolution. For the actuators shown in this manuscript, the cost of PVA per design at 20% fill density is about US$ 1.2 (9gm@100 USD per 750g). Thus, despite being non-reusable, the use of PVA as a sacrificial negative is cost-effective.

VI. Conclusion and Future Work

A novel fabrication method for fabricating soft pneumatic actuators was demonstrated. The technique uses PVA as a sacrificial negative mold for the fabrication of the first stage, i.e the pneumatic channel. The novel fabrication technique uses embedded endostructures to control the macroscopic bending characteristics of the actuators demonstrated here. The endostructures provide versatility for fabrication, as they can be made of a multitude of materials, even composites, with varying mechanical properties.

Thus, we propose a method in which all the required components apart from the silicone actuator can be FDM 3D printed, enabling affordable and easy fabrication without the need for specialized machinery or human skill. 3D printing ensures good repeatability, with the silicone molding process the only part of the fabrication involving human effort. A future iteration will use injection methods to eliminate the human element all together enabling automated fabrication. We plan to extend this work with the use of this technique for the fabrication of more complex, multidimensional features, to achieve varied types of motion such as torsion and bending. Using a combination of a dissolvable negative and being able to embed programming endostructures will enable the fabrication of more complex geometries. In the future, we are working on extending this idea to multidimensional endostructures, to enable three dimensional (non-planar) motions. We see applications for these actuators in the design of bio-inspired robots for locomotion as well as in grasping tasks. In addition, these robots can be used for wearable assistive devices, as the controlled compliance characteristics provide a basis for designs that can be customized to the end user's body.

VII. Acknowledgements

This work is supported by a National Robotics Programme - Robotics Enabling Capabilities and Technologies grant (R-261-506-027-305) awarded to RY. We thank the NUS Graduate School for Integrative Sciences and Engineering for providing scholarship support to AB.

References

[1] H. K. Yap, "Design , Fabrication , And Characterization Of Soft Pneumatic Actuators Towards Soft Wearable Robotic Applications," Ph.D. dissertation, National University of Singapore, 2017.

[2] G. Agarwal, N. Besuchet, B. Audergon, and J. Paik, "Stretchable Materials for Robust Soft Actuators towards Assistive Wearable Devices," *Scientific Reports*, vol. 6, no. October, 2016. [Online]. Available: http://dx.doi.org/10.1038/srep34224

[3] R. K. Katzschmann, "Building and Controlling Fluidically Actuated Soft Robots : From Open Loop to Model-based Control," Ph.D. dissertation, 2018.

[4] Y. Chen, S. Le, Q. C. Tan, O. Lau, F. Wan, and C. Song, "A reconfigurable hybrid actuator with rigid and soft components," in *Proceedings - IEEE International Conference on Robotics and Automation*. IEEE, may 2017, pp. 58–63. [Online]. Available: http://ieeexplore.ieee.org/document/7988691/

[5] S. Wakimoto, K. Suzumori, and K. Ogura, "Miniature pneumatic curling rubber actuator generating bidirectional motion with one air-supply tube," *Advanced Robotics*, vol. 25, no. 9-10, pp. 1311–1330, 2011.

[6] C. Mosadegh, P. Polygerinos, C. Keplinger, S. Wennstedt, R. F. Shepherd, U. Gupta, J. Shim, K. Bertoldi, C. J. Walsh, and G. M. Whitesides, "Pneumatic Networks for Soft Robotics that Actuate Rapidly," *Advanced Functional Materials*, vol. 24, no. 15, pp. 2163–2170, 2014. [Online]. Available: http://nrs.harvard.edu/urn-3:HUL.InstRepos:25922120

[7] B. S. Homberg, R. K. Katzschmann, M. R. Dogar, and D. Rus, "Haptic identification of objects using a modular soft robotic gripper," in *IEEE International Conference on Intelligent Robots and Systems*, vol. 2015-Decem. IEEE, 2015, pp. 1698–1705. [Online]. Available: http://eprints.whiterose.ac.uk/95166/

[8] W. H. Goh and M. Hashimoto, "Dual sacrificial molding: Fabricating 3D microchannels with overhang and helical features," *Micromachines*, vol. 9, no. 10, pp. 1–12, 2018.

[9] A. Koivikko and V. Sariola, "Fabrication of Soft Devices with Buried Fluid Channels by Using Sacrificial 3D Printed Molds," in *IEEE International Conference on Soft Robotics (RoboSoft)*, 2019, pp. 509–513.

[10] H. Zhao, Y. Li, A. Elsamadisi, and R. Shepherd, "Scalable manufacturing of high force wearable soft actuators," *Extreme Mechanics Letters*, vol. 3, pp. 89–104, 2015. [Online]. Available: http://dx.doi.org/10.1016/j.eml.2015.02.006

[11] L. Y. Zhou, Q. Gao, J. Z. Fu, Q. Y. Chen, J. P. Zhu, Y. Sun, and Y. He, "Multimaterial 3D Printing of Highly Stretchable Silicone Elastomers," *ACS Applied Materials and Interfaces*, vol. 11, no. 26, pp. 23 573–23 583, 2019. [Online]. Available: https://pubs.acs.org/doi/10.1021/acsami.9b04873.

[12] E. Steltza, A. Mozeikaa, J. Rembisza, N. Corsona, and H.MJaeger, "Jamming as an Enabling Technology for Soft Robotics," *Electroactive Polymer Actuators and Devices*, vol. 7642, 2010.

[13] Y. Wei, Y. Chen, T. Ren, Q. Chen, C. Yan, Y. Yang, and Y. Li, "A Novel, Variable Stiffness Robotic Gripper Based on Integrated Soft Actuating and Particle Jamming," *Soft Robotics*, vol. 3, no. 3, pp. 134–143, 2016.

[14] M. A. Robertson and J. Paik, "New soft robots really suck: Vacuum-powered systems empower diverse capabilities," *Science Robotics*, vol. 2, no. 9, pp. 1–12, 2017.

[15] J. W. Booth, D. Shah, J. C. Case, E. L. White, M. C. Yuen, O. Cyr-Choiniere, and R. Kramer-Bottiglio, "OmniSkins: Robotic skins that turn inanimate objects into multifunctional robots," *Science Robotics*, vol. 3, no. 22, p. 1853, 2018. [Online]. Available: http://robotics.sciencemag.org/

[16] P. Polygerinos, Z. Wang, J. T. Overvelde, K. C. Galloway, R. J. Wood, K. Bertoldi, and C. J. Walsh, "Modeling of Soft Fiber-Reinforced Bending Actuators," *IEEE Transactions on Robotics*, vol. 31, no. 3, pp. 778–789, 2015. [Online]. Available: http://ieeexplore.ieee.org.

[17] T. Tarvainen and W. Yu, "Pneumatic Multi-Pocket Elastomer Actuators for Metacarpophalangeal Joint Flexion and Abduction-Adduction," *Actuators*, vol. 6, no. 3, p. 27, 2017. [Online]. Available: http://www.mdpi.com/2076-0825/6/3/27

[18] F. Connolly, P. Polygerinos, C. J. Walsh, and K. Bertoldi, "Mechanical Programming of Soft Actuators by Varying Fiber Angle," *Soft Robotics*, vol. 2, no. 1, pp. 26–32, 2015.

[19] F. Connolly, J. Walsh, K. Bertoldi, and D. A. Weitz, "Automatic design of fiber-reinforced soft actuators for trajectory matching," *PNAS*, vol. 114, no. 1, pp. 51–56, 2017. [Online]. Available: www.pnas.org/cgi/doi/10.1073/pnas.1615140114

[20] A. Rafsanjani, Y. Zhang, B. Liu, S. M. Rubinstein, and K. Bertoldi, "Kirigami skins make a simple soft actuator crawl," *Science Robotics*, vol. 3, no. 15, p. eaar7555, 2018. [Online]. Available: http://robotics.sciencemag.org/lookup/doi/10.1126/scirobotics.aar7555

[21] Y. Sun, H. K. Yap, X. Liang, J. Guo, P. Qi, M. H. Ang, and C. H. Yeow, "Stiffness Customization and Patterning for Property Modulation of Silicone-Based Soft Pneumatic Actuators," *Soft robotics*, vol. 4, no. 3, pp. 251–260, 2017. [Online]. Available: https://www.researchgate.net/publication/317699843

[22] Y. Yang, Y. Chen, Y. Li, M. Z. Chen, and Y. Wei, "Bioinspired robotic fingers based on pneumatic actuator and 3D printing of smart material," *Soft Robotics*, vol. 4, no. 2, pp. 147–162, 2017.

[23] J. Santoso, E. H. Skorina, M. Salerno, S. De Rivaz, J. Paik, and C. D. Onal, "Single chamber multiple degree-of-freedom soft pneumatic actuator enabled by adjustable stiffness layers," *Smart Materials and Structures*, vol. 28, no. 3, pp. 1–21, 2019.

[24] L. Cappello, K. C. Galloway, S. Sanan, D. A. Wagner, R. Granberry, S. Engelhardt, F. L. Haufe, J. D. Peisner, and C. J. Walsh, "Exploiting Textile Mechanical Anisotropy for Fabric-Based Pneumatic Actuators," *Soft Robotics*, vol. 00, no. 00, p. soro.2017.0076, 2018. [Online]. Available: http://www.liebertpub.com/doi/10.1089/soro.2017.0076

[25] Y. Elsayed, A. Vincensi, C. Lekakou, T. Geng, C. M. Saaj, T. Ranzani, M. Cianchetti, and A. Menciassi, "Finite Element Analysis and Design Optimization of a Pneumatically Actuating Silicone Module for Robotic Surgery Applications," *Soft Robotics*, vol. 1, no. 4, pp. 255–262, 2014.

[26] P. Moseley, J. M. Florez, H. A. Sonar, G. Agarwal, W. Curtin, and J. Paik, "Modeling, Design, and Development of Soft Pneumatic Actuators with Finite Element Method," *Advanced Engineering Materials*, vol. 18, no. 6, pp. 978–988, 2016.

[27] S. Sareh, K. Althoefer, M. Li, Y. Noh, F. Tramacere, P. Sareh, B. Mazzolai, and M. Kovac, "Anchoring like octopus: Biologically inspired soft artificial sucker," *Journal of the Royal Society Interface*, vol. 14, no. 135, 2017. [Online]. Available: http://dx.doi.org/10.1098/rsif.2017.0395